DOI 10.1007/s11041-022-00810-0
Metal Science and Heat Treatment, Vol. 64, Nos. 5 – 6, September, 2022 (Russian Original Nos. 5 – 6, May – June, 2022)

UDC 669.1.17

PATTERNS OF THE FORMATION OF REDUCED HARDNESS ZONES IN A WELDED JOINT OF RAILWAY RAILS

R. A. Shevchenko,[1] A. B. Yur'ev,[1] N. A. Kozyrev,[1] and A. R. Mikhno[1]

Translated from *Metallovedenie i Termicheskaya Obrabotka Metallov*, No. 6, pp. 40 – 46, June, 2022.

Original article submitted December 24, 2021.

The research investigates the structure of a welded joint of a railway rail after local heat treatment and without it. Macro- and microstructural analyses of rail samples were performed using optical microscopy methods. The hardness of the rail running surface in the heat-affected zone of butt welds was measured. It has been found that the formation of zones with reduced hardness is inevitable due to the temperature gradient created during the welding process. Moreover, using local induction heat treatment results in the formation of new, more extended zones with reduced hardness. It has been determined that the only solution to this problem is to reduce the extent of heat-affected zones to sizes that do not lead to increased wear and local crushing.

Keywords: flash butt welding; rail steel; heat-affected zone; microstructure; hardness.

INTRODUCTION

Currently, the warranty operating time for rails according to All-Union State Standard (GOST) 51685–2013 is in the range 320 to 500 million gross tons depending on their category and the radius of curved track sections. At the same time, in 2014 there was a transition from rails of the VT category (volumetrically thermally hardened) to rails which are differentially hardened from rolling heating with a minimum hardness of 350 *HB*. As a result, two domestic plants produce 100-m long DT350 rails with a predicted service life of 1.1 billion gross tons [1].

According to future plans, an increase in the service life of rails to 1.5 billion gross tons is expected in order to reduce the infrastructure maintenance specific costs by 20 – 30% [2]. At the same time, rail welding enterprises in conformity with the 1.08.002–2009 technical requirements of Russian Railways (RZhD) guarantee the operating time of welded rail joints of 150 million gross tons, which is 47% of the minimum requirement for warranty operating time of rails. It also comprises 21% of the demonstrated resources totalling 700 million gross tons. Consequently, a considerable share of the cost items for the current track maintenance is the maintenance of welded joints. Moreover, the primary task of reducing costs is to increase the operational life of welded joints of rails made by electric-contact welding.

In the process of manufacturing a continuous welded rail track during rail welding, obligatory local heat treatment of the butt weld is used [3, 4]. Heat treatment of welds includes hardening of the running surface of the rail head and normalization of the rail base and web, which makes it possible to increase the strength characteristics of welded rail joints [5]. Heat treatment is carried out with the help of induction heat treatment installations. With all the positive effects of heat treatment using forced air as a quenching medium, modern induction installations also have several disadvantages. Among them, the following can be noted: (*1*) the appearance of new heat-affected zones (HAZ) during local heating of welded joints during heat treatment; (*2*) one-sided (only from the side of the head) cooling, which leads to a deterioration in the straightness of the welded joints after cooling; (*3*) insufficient depth of weld heating during heat treatment.

Local heat treatment of a butt weld leads to an increase in the number of and the appearance of new HAZs as compared to the zones during welding of rails by the electric-contact method without heat treatment [6]. An increase in the HAZ linear dimension in the rail head at about 40 – 47 mm and in its base at 70 – 75 mm from the butt weld caused by heat treatment results in a decrease in the mechanical properties of the welded joint [7].

[1] Siberian State Industrial University, Novokuznetsk, Russia (e-mail: kozyrev_na@mtsp.sibsiu.ru).

0026-0673/22/0506-0332 © 2022 Springer Science+Business Media, LLC

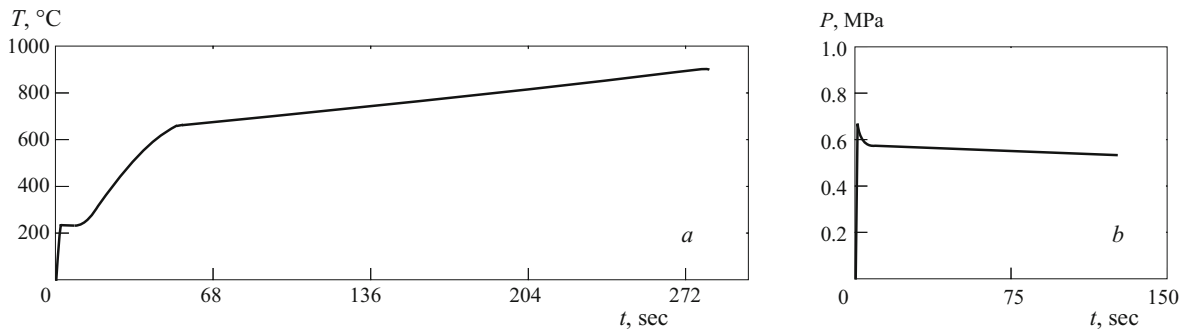

Fig. 1. Tempering mode of the welded joint sample: *a*) heating for induction hardening; *b*) cooling with forced air (under pressure *P*).

As a result, increased local wear of the head running surface, crushing, and chipping are observed in the reduced hardness zone. This defect type (i.e. crushing of the rail head due to uneven mechanical properties of the metal at the butt weld) leads to large economic losses during the operation of railway tracks. It is of practical and scientific interest to establish the cause of this defect and develop methods for its elimination [2, 8].

The paper aims to study the patterns of forming reduced hardness zones in welded joints of railway rails in the initial state and after local induction heat treatment.

METHODS OF STUDY

For the study, two samples of full-profile rails of the R65 type of the DT350 category with a length of at least 600 mm were cut out. The samples had a chemical composition corresponding to rail steel 76KhSF (0.71 – 0.82% C; 0.75 – 1.25% Mn; 0.25 – 0.60% Si; 0.50 – 1.25% Cr; 0.08 – 0.15% V; < 0.02% P; < 0.02% S; < 0.02% Al) (GOST 51685–2013). The flash butt welding of the rails was performed on an MSR-6301 electric welding machine according to a chosen mode which corresponded to the modes of the 1.08.002–2009 technical requirements of RZhD “Railway rails welded by an electric-contact method” (see Table 1).

After welding, sample *A* of the rail joint was subjected to local induction heat treatment (LIHT) on a UIN 001-100/RT-S stationary induction heater designed for heat treatment of welded rail joints according to the modes shown in Fig. 1. Sample *B* was examined in the initial state (i.e. without LIHT).

For the macrostructure test, deep etching of templates was performed. For this purpose, we immersed them with the controlled surface upwards into a 50% aqueous solution of hydrochloric acid with a density of 1.19 ± 0.005 g/cm^2 in a heated state (up to 70 ± 10°C). The acid solution layer above the controlled surface was at least 20 mm.

The microstructure of rail butt welds was studied using an OLYMPUS GX-51 optical microscope. Etching was performed in 4% nital.

TABLE 1. R65 Rail Welding Modes

Parameter	The value of the parameter in flashing-off sections/melting zones									
	1	*2*	*3*	*4*	*5*	*6*	*7*	*8*	*9*	*10*
S, mm	2	4	3	2.5	2.5	2	1.5	1.5	1.5	1.5
U, %	75	70	55	60	60	65	70	88	88	98
V_c, mm/sec	0.6	1.3	0.8	1	1.1	1.2	0.7	0.9	1.1	1.2
V_a, mm/sec	0.5	0.6	0.5	0.5	0.4	0.4	0.5	0.4	0.3	0.2
I_{cor}, A	200	300	200	200	250	250	250	300	400	500
I_{stop}, A	300	450	350	350	400	400	460	500	600	700
I_{rev}, A	400	500	400	400	450	450	550	600	700	800
I_{sc}, A	1200	1200	1200	1200	1200	1200	1200	1200	1200	1200

Notations: *1*, *2*, *3*, ..., *10*) the number of the melted zone where the appropriate values for the melting path *S* and primary voltage *U* given as a percentage of the mains voltage (380 V) were determined; V_c and V_a are the speed of converging and diverging the welded rails respectively; I_{cor}, I_{stop}, I_{rev} indicate the current in the primary transformer winding at which rails are moved closer, are not moved, are moved apart; I_{sc} is the short-circuit current intensity which must not be reached.

Note. Precipitation path S_{pr} = 14 mm; precipitation velocity v_{pr} = 100 mm/sec; precipitation path in current S_I = 6 mm.

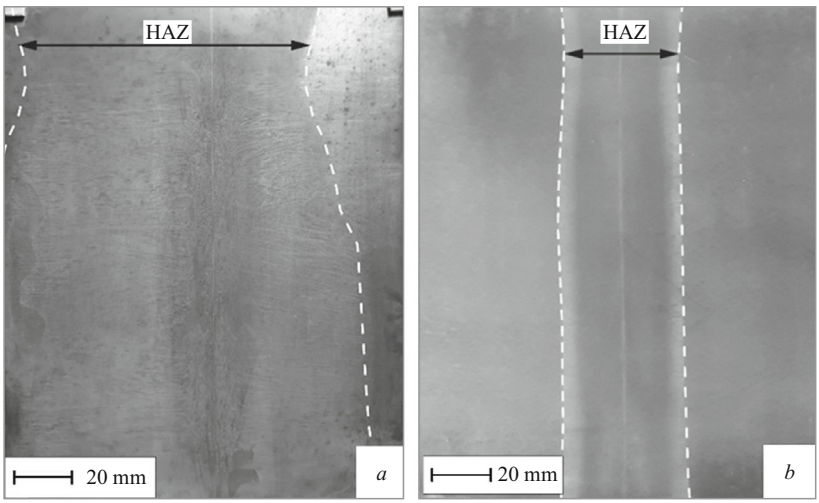

Fig. 2. Microstructure of the longitudinal macrotemplates of the welded joints: *a*) sample *A*; *b*) sample *B*.

To assess the change in hardness along extent of the LIHT heat-affected zone, an UZIT-3 ultrasonic hardness tester manufactured according to technical specifications 427-002-20872624–00 was used.

RESULTS

The analysis of the macrostructure of the welded joint metal subjected to LIHT after welding (sample *A*, Fig. 2*a*) showed that a dark-etched uneven HAZ is observed on both sides of the weld. The heat-affected zone had the following linear dimensions (on one side of the seam): in the head — 51 mm, in the web — from 45 to 62 mm, in the base — 64 mm. No shatter cracks were found in the HAZ and the seam.

On the longitudinal macrotemplate of sample *B* (Fig. 2*b*), there is a uniform HAZ obtained after welding. Along the entire length of the joint, the HAZ width is (on one side of the joint) 22 mm. No shatter cracks were detected in the metal.

The welding zone of sample *A* (after LIHT) consists of fusion and heat affected zones. The fusion zone up to 0.5 mm wide has the structure of fine-lamellar pearlite and grain boundary ferrite (Fig. 3*a*) with grain sizes corresponding to No. 8 according to the GOST 5639–82 scale. Such a structure is characteristic of normalized steel. The fusion zone is followed by a section that has the structure of fine-lamellar pearlite with ferrite precipitates (Fig. 3*b*). The structure of the metal in the softening zone (a zone with reduced hardness) at a distance of over 10 mm from the butt weld is sorbitic and granular pearlite in various coagulation stages (Fig. 3*c* – *e*). The softening zone is located at 10 – 40 and 10 – 70 mm from each of the two sides of the butt weld, respectively. Further, in the base metal zone, there is a decrease in the content of granular and an increase in the proportion of lamellar pearlite (Fig. 3*f*).

The weld zone of sample *B* (without LIHT) as well as of sample *A* consists of fusion and heat affected zones. The fusion zone of up to 3 mm in width has the structure of large-lamellar pearlite and grain-boundary ferrite (Fig. 4*a*) with grain sizes corresponding to No. 4 – 3 according to the GOST 5639–82 scale. There is a zone of up to 5 mm in width next to the fusion zone. It has a coarse-grained structure consisting of lamellar pearlite (without ferrite precipitates) formed due to overheating and recrystallization of the metal (Fig. 4*b*). A fine-grained zone (Fig. 4*c*) with a width of about 10 mm follows the coarse-grained structure zone. This was formed due to metal recrystallization. The grain size in this zone corresponds to No. 8 – 9 according to the GOST 5639–82 scale. In the zone at the boundary between the HAZ and the base metal (at a distance of 15 – 20 mm from the fusion zone), the microstructure consists mainly of granular pearlite, which is typical for the state after tempering (Fig. 4*d*). Further, the structure of the base metal, i.e. lamellar pearlite, is observed (Fig. 4*e*).

The hardness of the butt weld metal and the HAZ on the running surface of the head of butt weld *A* varies from 265 to 318 *HB*, and that of weld B varies from 292 to 355 *HB*. Fig. 5 shows the change in the hardness of the metal along the running surface of the butt weld. The hardness of the base metal on the running surface of the head is 348 – 354 *HB*.

The decrease in the hardness of the metal of the head in the HAZ of butt weld *A* relative to the lower limit of the base metal hardness of the rail reaches 24.5%. The extent of the reduced hardness zone is 42 mm. The decrease in the hardness in the HAZ of butt weld B reaches 14.8%, while the extent of the zone with reduced hardness is 14 mm.

DISCUSSION

It is known that a decrease in hardness in the HAZ in rails made of pearlitic steel is associated with the formation of granular pearlite [9, 10], but as a rule, its formation patterns are not discussed. This phenomenon is often seen as an obvious consequence of the heat input during welding.

The formation of areas with reduced hardness during welding is similar to the spheroidizing annealing process

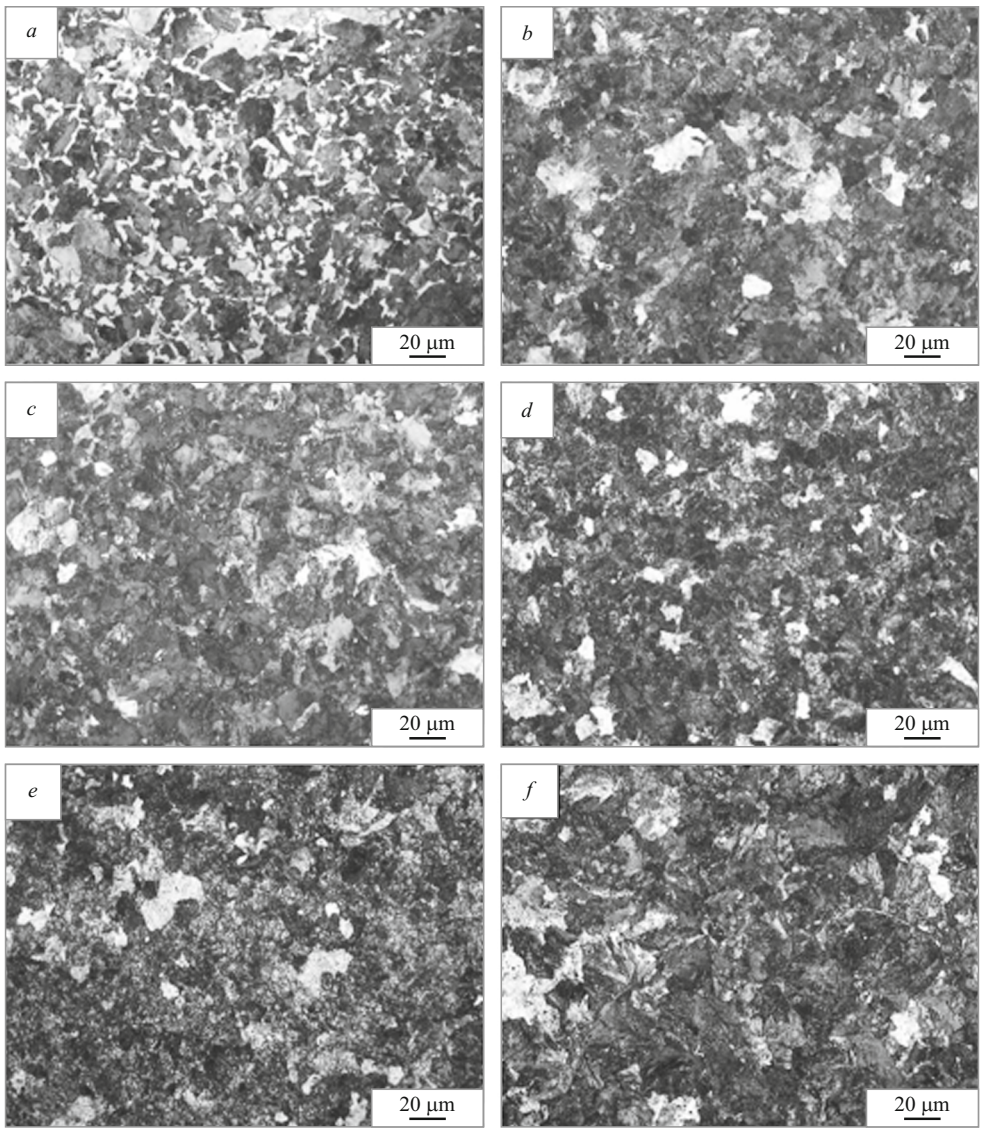

Fig. 3. Microstructure in different zones of the welded joint of sample *A*: *a*) butt weld; *b*, *c*, *d*, *e*) at a distance of 2.5; 10; 10 – 40; 40 – 60 mm from the butt weld, respectively; *f*) base metal.

used in production to reduce hardness and improve the machinability of steels by cutting. To obtain granular pearlite (globular cementite), spheroidizing annealing of steel is performed. The process consists in heating the sample to a temperature slightly above the *PSK* line (critical point Ac_1), holding, and subsequent cooling. Initial austenite nuclei are formed by dislocation when heated somewhat above Ac_1 while maintaining coherent grain boundaries. The austenite nucleus appears at the interface between ferrite and cementite (Fig. 6). As a result of this transformation, low-carbon austenite is formed. Cementite dissolves in the low-carbon austenite formed by dislocation mechanism, and the carbon content in austenite approaches the equilibrium content. The growth of austenite regions following the polymorphic $\alpha \rightarrow \gamma$ transformation proceeds faster than the dissolution of cementite. Excess structural components do not completely pass into solution and, upon subsequent cooling, are centers of cementite spheroidization (Fig. 6).

The introduction of chromium, vanadium, molybdenum, tungsten, and other carbide-forming elements into steel delays the austenitizing process due to the formation of alloyed cementite or alloying element carbides which are less soluble in austenite [11 – 14].

Cementite coagulation in the areas of the remaining undissolved carbide and cementite grain coarsening (i.e. spheroidization) occur during subsequent cooling. Fig. 6 is a diagram of two types of eutectoid transformations resulting in the formation of granular or lamellar pearlite.

Pearlite fineness depends on the steel composition and cooling conditions. Slow cooling contributes to the coarsening of carbides and vice versa. The cooling rate affecting diffusion transformations causes a significant effect on the

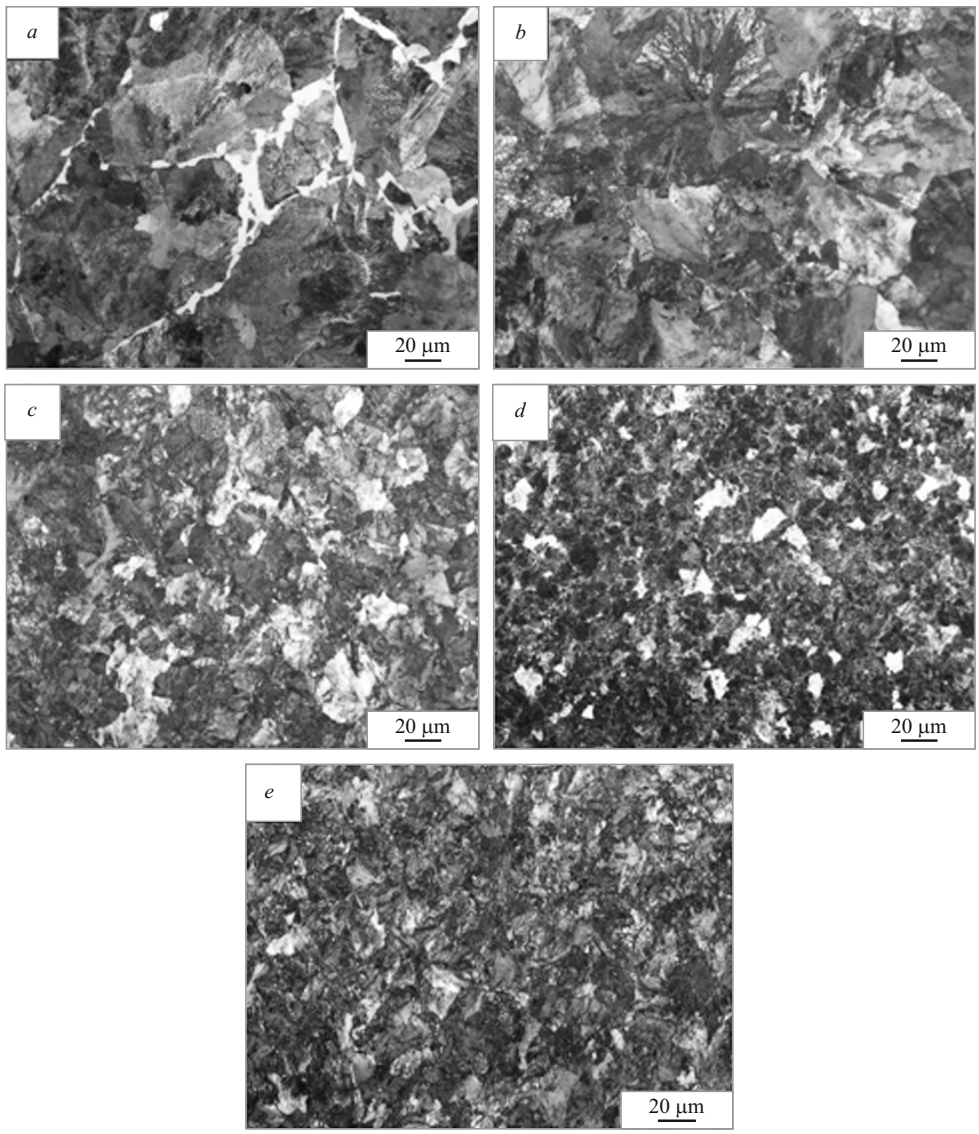

Fig. 4. Microstructure in different zones of the welded joint of sample *B*: *a*) butt weld; *b*, *c*, *d*) at a distance of 2.5; 10; 20 mm from the butt weld, respectively; *e*) base metal.

structure and properties of the ferrite/cementite mixture which is formed during austenite decomposition. During rail welding, the formation of granular pearlite occurs in the areas whose temperature reaches the values ranging between the critical points Ac_1 and Ac_m.

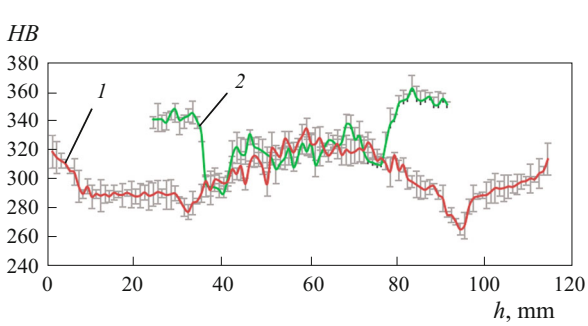

Fig. 5. Hardness distribution of the metal on the running surface of butt welds in the longitudinal direction (*h* is the distance from the beginning of the measurement): *1*) Sample *A*; *2*) Sample *B*.

CONCLUSIONS

The research investigated welded joint samples of railway rails in the initial state and after local induction heat treatment. It has been shown that reduced hardness zones appear in the areas of metal heating in the $Ac_1 - Ac_m$ temperature range where complete dissolution of carbides does not occur. Subsequently, these carbide particles are the centers of cementite spheroidization.

As a result of studying the patterns of forming zones with reduced hardness in a welded joint, it has been found that their appearance is inevitable due to the presence of a

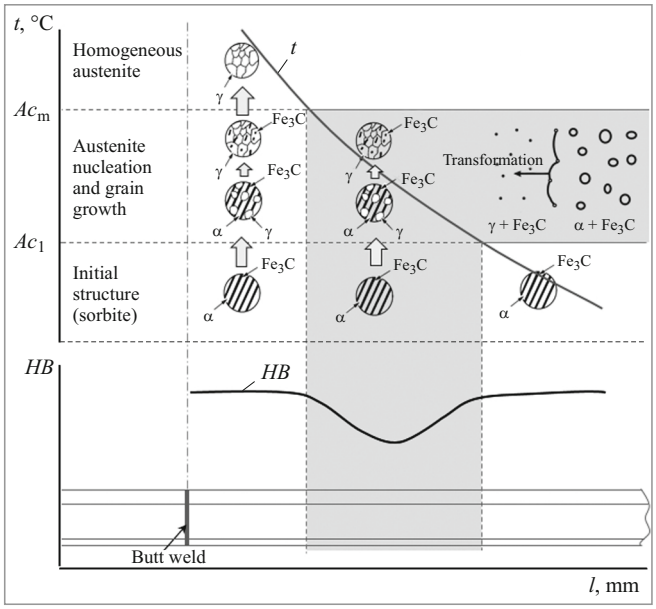

Fig. 6. Diagram of forming heat-affected zones of reduced hardness during welding and local heat treatment of railroad rails and changing the temperature (t) and hardness (HB) along the length of the rail: l) the distance from the butt weld in the longitudinal direction.

temperature gradient created during welding. The use of local heat treatment of a welded joint of railway rails makes it possible to recrystallize the weld metal, reduce the grain size, and break the formed ferrite network into separate sections. However, heat treatment leads to the appearance of new, more extended heat-affected zones with reduced hardness than after welding rails by electric-contact welding without heat treatment. During the operation of rails which were heat-treated in the welding zone, there is increased wear of their running surface and head crushing at the butt weld, which causes premature removal of such rails from service.

Existing methods of welding railway rails and local heat treatment of butt welds do not make it possible to eliminate reduced hardness zones. The only solution to this problem is to reduce the extent of heat-affected zones to sizes that do not lead to increased wear and local crushing of these areas.

The study was performed with the financial support of the Russian Foundation for Basic Research and Kemerovo Oblast within the framework of scientific project No. 20-48-420003r_a "Developing the physicochemical and technological foundations for creating a fundamentally new method of welding differentially heat-strengthened railway rails."

REFERENCES

1. V. V. Chesnokov, "The keynote speech by the Chief engineer of the East Siberian infrastructure directorate," in: *Improving the Quality and Operating Conditions of Rails and Rail Fasteners (Based on the Meeting of the Non-Commercial Partnership "Rail Commission," September 7 – 9, 2016), Collection of Scientific Reports* [in Russian], UIM, Ekaterinburg (2016), pp. 10 – 11.
2. A. I. Lisitsyn and I. A. Kuznetsov, "An analysis of the operation of rails of new categories on the Russian railway network and promising lines of work to improve their reliability," in: *Improving the Quality and Operating Conditions of Rails and Rail Fasteners (Based on the Meeting of the Non-commercial Partnership "Rail Commission," 7 – 9 September 2016), Collection of Scientific Reports* [in Russian], UIM, Ekaterinburg (2016), pp. 15 – 23.
3. V. A. Rezanov, *Developing a Flash Method for Resistance Welding of Alloyed Rails, Author's Abstract of Candidate's Thesis* [in Russian], Moscow (2013), 140 p.
4. N. A. Kozyrev, R. A. Shevchenko, A. A. Usoltsev, et al., "Developing and modeling the technological process of welding differentially heat-strengthened railway rails. Modeling of processes occurring during welding and local heat treatment," *Izv. Vysh. Uchebn. Zaved., Chern. Metall.,* **63**(2), 93 – 101 (2020).
5. P. E. Sazonov, "Specific features of welding new types of rails of the DT350, DT370IK categories," in: *Improving the Quality and Operating Conditions of Rails and Rail Fasteners (Based on the Meeting of the Non-commercial Partnership "Rail Commission," September 25 – 27, 2015), Collection of Scientific Reports* [in Russian], UIM, Chelyabinsk (2015), pp. 189 – 192.
6. A. I. Nikolin, *Improving the Processes of Welding and Heat Treatment of Rails of Trunk Railways, Author's Abstract of Candidate's Thesis* [in Russian], Moscow (2004), 200 p.
7. S. I. Zhuravlyov, A. Ya. Sudarkin, L. S. Sergeyev, and A. B. Korolyova, "Technological capabilities of smart equipment for flash butt welding," *Svarka Diagnost.,* No. 3, 51 – 56 (2009).
8. A. I. Lisitsyn, "Current requirements for rail products supplied for OJSC Russian Railways," in: *Improving the Quality and Operating Conditions of Rails and Rail Fasteners (Based on the Meeting of the Non-Commercial Partnership "Rail Commission," September 25 – 27, 2015), Collection of Scientific Reports* [in Russian], UIM, Chelyabinsk (2015), pp. 84 – 94.
9. G. Girsch, J. Keichel, R. Gehrmann, et al., *"*Advanced rail steels for heavy haul application-track performance and weldability,*" in: Heavy Haul Conf., Shanghai, China, June 22 – 25* (2009), pp. 171 – 178.
10. P. Mutton, J. Cookson, C. Qui, and D. Welsby, "Microstructural characterisation of rolling contact fatigue damage in flashbutt welds," *Wear*, **366**, 368 – 377 (2016).
11. Yu. M. Lahtin, V. P. Leontiev, *Materials Science, Textbook for Technical Higher Education Institutions* [in Russian], Mashinostroyeniye, Moscow (1990), 528 p.
12. T. Oyama, O. D. Sherby, J. Wadsworth, and B. Walser, *Scr. Metall.*, **18**, 799 – 804 (1984).
13. T. Nakano, H. Kawatani, S. Kinoshita, *Trans. Iron Steel Inst. Jpn*, **17**, 110 – 115 (1977).
14. G.-H. Zhang, J.-Y. Chae, K.-H. Kim, and D. W. Suh, *Mater. Charact.*, **81**, 56 – 67 (2013).